Advances in Science and Technology Research Journal

Advances in Science and Technology Research Journal 2021, 15(3), 197–214
https://doi.org/10.12913/22998624/138924
ISSN 2299-8624, License CC-BY 4.0

Received: 2021.06.14
Accepted: 2021.07.20
Published: 2021.08.16

Fire Detection Methods Based on Various Color Spaces and Gaussian Mixture Models

Amr A. Munshi[1*]

[1] Computer Engineering Department, Umm Al-Qura University, Saudi Arabia
* Corresponding author's email: aaamunshi@uqu.edu.sa

ABSTRACT
Fire disasters are very serious problems that may cause damages to ecological systems, infrastructure, properties, and even a threat to human lives; therefore, detecting fires at their earliest stage is of importance. Inspired by the technological advancements in artificial intelligence and image processing in solving problems in different applications, this encourages adopting those technologies in reducing the damage and harm caused by fire. This study attempts to propose an intelligent fire detection method by investigating three approaches to detect fire based on three different color models: RGB, YCbCr, and HSV were presented. The RGB method is applied based on the relationship among the red, green and blue values of pixels in images. In the YCbCr color model, image processing and machine learning techniques are used for morphological processing and automatic recognition of fire images. In turn, for HSV, supervised machine learning techniques are adopted, namely decision rule and Gaussian mixture model (GMM). Further, the expectation maximization (EM) algorithm was deployed for the GMM parameters estimation. The three proposed models were tested on two data sets, one of which contains fire images, the other consists of non-fire images with some having fire-like colors to test the efficiency of the proposed methods. The experimental results showed that the overall accuracies on two data sets for the RGB, YCbCr, and HSV methods were satisfactory and were efficient in detecting the outdoor and indoor fires.

Keywords: fire detection; fire pixels; fire-like pixels; color models; Gaussian mixture models.

INTRODUCTION

Fire disasters are serious problems around the world. In order to predict fire disasters, various methods have been used to detect fires, such as fire watch towers, physical sensors, satellite and aerial monitoring, and video and digital image analysis. The reliability of fire watch tower depends greatly on the operator's assessment. Physical sensors, which are often based on particle sampling, temperature sampling, relative humidity sampling, air transparency testing, and smoke analysis, can cause false alarms, for example, individual smoking nearby or vapor from the cooking process. Moreover, reliability of this fire detection system depends on the distribution of sensors; and the fire location, its size as well as growing rate cannot be determined. Therefore, this kind of detection is only suitable to close and small areas. Meanwhile, the satellite and aerial monitoring system is very expensive and can be activated when the fire has already spread significantly.

There has been a continuous interest in conducting the studies related to fire detection based on video and image analysis. Most of the work in fire detection in color images and videos are based on setting color rules. [1, 2] proposed a method of developing a set of rules for fire pixel classification based on video image processing. The RGB color system was used to extract fire pixels and smoke pixels, which are then verified if they are real fire pixels or fire-like pixels. [3, 4] attempted to detect fires and flames by processing the video data generated by an ordinary camera monitoring a scene. The fire pixels are determined by ordinary motion, RGB color clues, and video analysis in the wavelet domain.

[5] proposed an approach to detect fires in real time by combining the foreground object information with color pixels statistics of fire based on the RGB color system. Other methods utilize threshold selection and image feature analysis for early fire detection [6]. An adaptive background subtraction algorithm was developed to extract the foreground information, then this foreground region was verified to determine if it is a fire candidate or not. The algorithm was the developed [7] utilizing a YCbCr color space, since it can separate the illumination information from chrominance more efficiently than other color space. [8] used flame contours for early fire detection from video sequences. The process of fire detection consists of candidate fire frame selection, flame region selection, and flame contour-based fire decision. [9] utilized the RGB color space to develop a set of rules to classify the fire pixels from images. Meanwhile, [10] proposed an approach in which the statistical fire color model (RGB) and sequential pattern mining technology are combined to detect fire in images.

Many studies have been conducted on detecting fire using the YCbCr color model as well. In a research conducted by [7], the YCbCr color system was utilized. The advantage of using such color system is the ability of separating the luminance from the chrominance more effectively than other color spaces. Then a generic chrominance model was proposed for flame pixel classification. This further alleviates the harmful effects of changing illumination and also detects fire more efficiently; moreover, higher accuracy rates were achieved by utilizing the YCbCr color system over the RGB color system. [11] also performed a research based on the color model approach, to classify a pixel to be fire the model identifies seven rules. If a pixel satisfies those seven rules, then it is classified as fire. In this method, two color systems namely, RGB and YCbCr were utilized in the classification process. However, this approach was limited to detecting forest fires, which hinders the usage of this approach.

Due to developments in digital image and video processing, also inspired by the artificial intelligence capabilities, computer vision-based fire alarm systems tend to replace the conventional detection systems [12, 14÷15]. These new systems can cover larger detection areas with higher reliability. Thus, exploring the approaches to detect fire based on color systems and the application of machine learning techniques is of interest.

The remainder of the paper is structured as follows. Section 2 presents the methodology to extract fire pixels from images; further, the results on a real-world dataset are presented. Section 3 presents a fire detection algorithm based the YCbCr color space and the results are evaluated on real images. The details of detecting fire regions based on an HSV color model and the decision rules to validate fire utilizing the Gaussian mixture model (GMM) are presented in Section 4. Finally, the conclusions are drawn.

The RGB Based Method

By studying the visual features of fire, it is can be observed that fires have unique visual features. These features can be divided into static and dynamic characteristics, which are both used in the classification of fire pixels. In terms of static characteristics, flames often have reddish colors and they will vary with an increase in temperature. When the fire is in its early stage, its temperature is low and the colors range from red to yellow. However, when the fire develops and reaches higher temperature, its color may turn into white. This means that a low-temperature flame emits a light with high saturation, whereas a high-temperature flame emits a low-saturation light. In addition, the saturation in the day-time or with background illumination is stronger than that of during the night-time or without light source. Accordingly, three color spectra of the segmented fire region exist namely, white-yellow, orange, and red. In terms of dynamic characteristics, the shape of the flame varies with time, because it could be affected by the wind. Furthermore, the fire becomes larger and larger if it is not extinguished; therefore, the area of the flame also varies. These properties are often utilized in the separation of the foreground (the flame) from the background in order to increase the reliability of the method.

In this section, the static characteristics of fires in the RGB color space to determine fire pixels in color images are deployed.

The RGB Color Space

The RGB color model [13] is based on a Cartesian coordinate system. The RGB model forms its gamut from the primary additive colors of red, green and blue. The combination of red, green and blue light in the same amounts forms white. Computers generally display RGB images using 24-bit

color. In the 24-bit RGB color model, there are 256 variations for each of the additive colors of red, green and blue. Therefore, there are 256 reds x 256 greens x 256 blues = 16,777,216 possible colors in the 24-bit RGB color model. In this color model, colors are represented by varying intensities of red, green and blue light. The intensity of each of the red, green and blue components is represented on a scale from 0 to 255 with 0 being the least intensity to the maximum intensity of 255.

The RGB Color Space Based Algorithm

The most important step of the implementation is to train data so that a model is constructed. This model should be able to verify if there were flames in the input images data. The training data, including the threshold (upper-bounds and lower-bounds) for the relationship of RGB values, were determined from the histograms of the region of interest (ROI) containing flame in each image. A dataset consisting of seventy images containing flames was utilized. Then, for this dataset, the ROI is determined and separated into three different color channels. Further, their histograms are studied in order to find the correlation among the RGB values and HSI values. The maximum, minimum, and mean values of each pixel of each color channel were observed. From the dataset, seventy sets of RGB were extracted. The histograms from those images consisting of flames were investigated to find out if any patterns exist. Figure 1 shows an example of a set of histograms obtained by extracting the ROI over the flames.

$$R(x,y) > G(x,y) > B(x,y) \quad (1)$$

where: (x,y) is the coordination of the pixel; R, G, B are the intensities of the pixel at location (x,y) respectively. For a fire pixel, the red-channel pixel has a higher value than the green channel pixel and the green-channel pixel value is greater than that of the blue channel.

Furthermore, the red-channel value and the green-channel value of a fire pixel are greater than 190 and 90, respectively; in turn, the blue-channel value of the same pixel is less than 140. This introduces the second condition:

$$R(x,y) > 190;\ G(x,y) > 90;\ B(x,y) < 140 \quad (2)$$

However, fire-like colors are sometimes misclassified as fire, leading to false alarms. As mentioned previously, both luminance (intensity) and chrominance changes in direct proportion to illumination. When a camera captures an image, the illumination it obtains from a flame is higher than that of a fire-like object, such as orange, rose, and red tiles. Therefore, the luminance and chrominance of flame are higher than those of fire-like objects. In order to overcome this, chromaticity

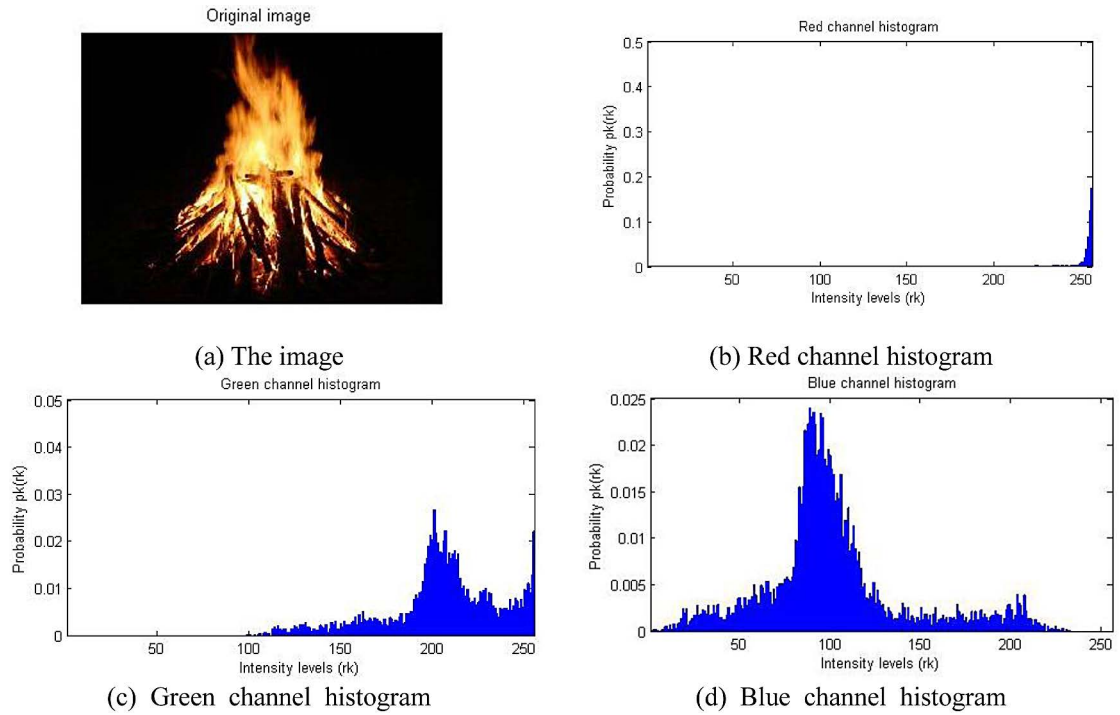

(a) The image (b) Red channel histogram

(c) Green channel histogram (d) Blue channel histogram

Fig. 1. Histograms of a region over the flame

is deployed. As the RGB colors contain the luminance and the chrominance of the pixels, it is desired to separate them. In order to accomplish this, two luminance and chrominance separation techniques are mentioned in the following sections. The third observed condition for classifying color-based fire should satisfy:

$$0.10 \leq \frac{G(x,y)}{R(x,y)+1} \leq 1.0$$

$$0.10 \leq \frac{\mathrm{B(x,y)}}{\mathrm{R(x,y)}+1} \leq 0.85 \qquad (3)$$

$$0.10 \leq \frac{B(x,y)}{G(x,y)+1} \leq 0.85$$

Accordingly, the pixels in images that satisfy the three inequalities (1), (2), and (3), are considered fire pixels. The flowchart of the presented method based on the RGB color model is illustrated in Figure 2.

In this method, an image is the input. The image is then separated into three color channels, namely the Red channel, the Green channel, and the Blue channel. Next, every pixel of the image is scanned to verify if it is a candidate fire pixel. If the RGB values of the scanned pixel satisfy the three inequalities, the pixel is classified as a fire pixel and labelled 1; otherwise, it is labelled 0 and the next pixel (if any) is scanned. Then, the binary image is morphologically processed to remove small objects and fill holes to improve the shape of the flame. Finally, once all the pixels of the image are scanned, if the number of detected fire pixels exceeds the threshold, the fire alarm is activated. In this setting, the threshold of fire pixels was set to 50, as small blobs of fire can contain over 50 pixels. The purpose of setting this threshold is to reduce the number of false alarms due to fire-like colors and hence increase the reliability of the method.

Results of RGB Color Space Based Algorithm

In order to verify the method, one hundred and forty images were collected, seventy of which contain fires or flames, the remaining images do not contain fire, but some images contain

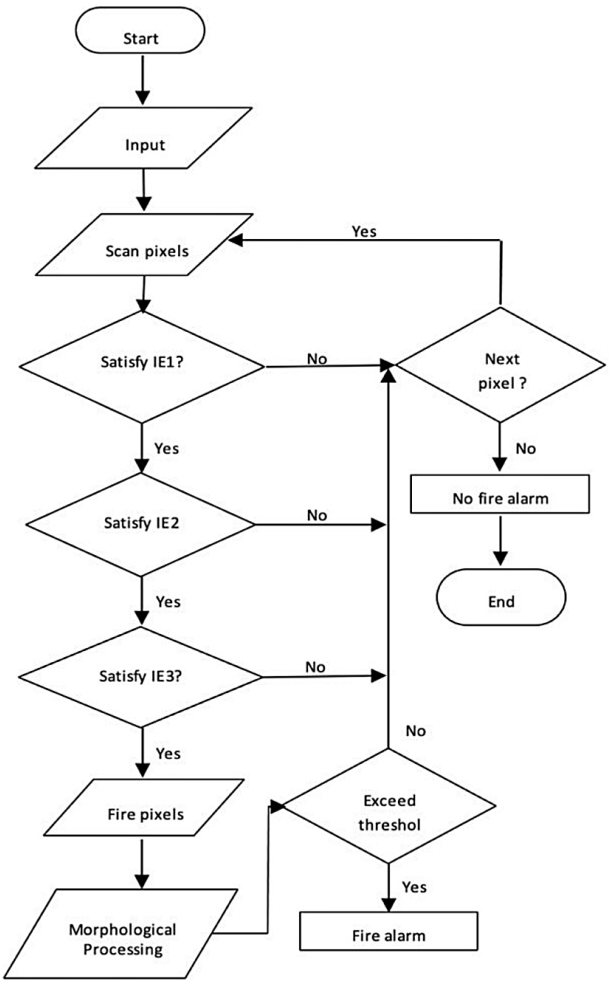

Fig. 2. Flowchart of the proposed method based on the RGB color model

fire-like colors. Each image was scanned using inequalities (1), (2), and (3) to determine if fire pixels exist in the image. Figure 3 shows fire pixel segmentations in the binary images when inequalities (1), (2) and (3) were applied. Figure 3(a) shows the original image; Figure 3(b) shows the binary image, in which the pixels satisfying inequality (1) are mapped to white; Figure 3 (c) demonstrates the resulting binary image when rules (1) and (2) were applied to the original image. The final image in Figure 3(d) is the result of the simultaneous application of rules (1)-(3), and morphological processing to segment fire pixels in the original image. The morphological processing removed objects with the number of pixels less than 50 and filled the other objects with additive pixels. It can be clearly seen that the more rules applied to the original image, the more similar the segmented flame to original flame. As can be seen from Figure 4, the dried leaves on the ground have a similar color to that of the flame; however, the image was not classified as a fire image because the three rules and morphological processing were unsatisfied.

However, there were some cases in which the images containing no flame but fire-like colors can be segmented as fire, even though three rules were all applied. Figure 4 shows the results when rule (1), rules (1) + rule (2), rule (1) + rule (2) + rule (3) were applied, respectively.

When the first set of images were tested, which contains seventy images of fire, 100% of the images were classified as fire. This means that the accuracy is 100%. However, when the algorithm was tested on the second set of data including some images having fire-like colors, false

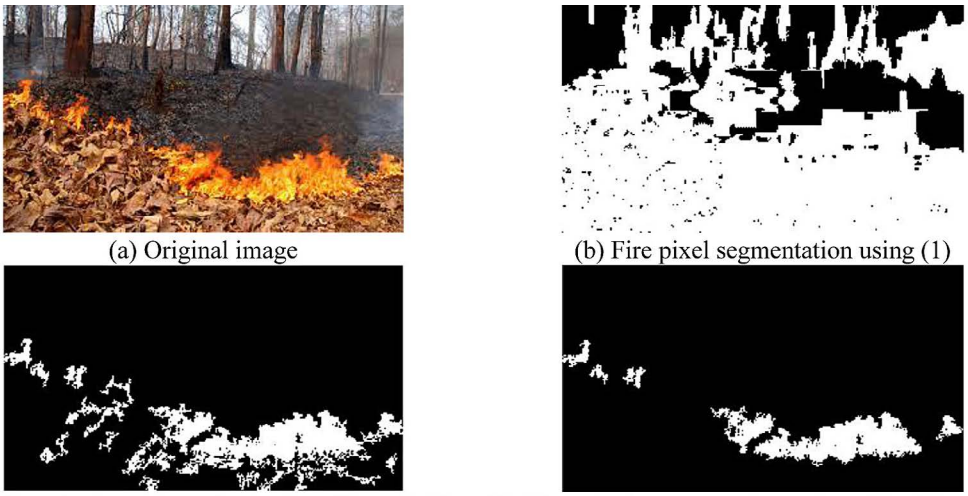

(a) Original image (b) Fire pixel segmentation using (1)

(c) Fire pixel segmentation using (1) and (2) (d) Fire pixel segmentation using (1), (2), and (3)

Fig. 3. Fire pixel segmentation

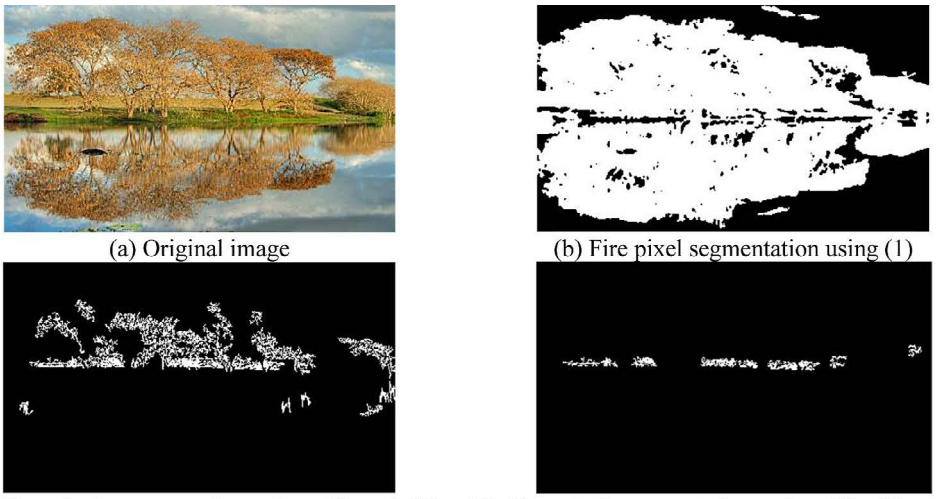

(a) Original image (b) Fire pixel segmentation using (1)

(c) Fire pixel segmentation using (1) and (2) (d) Fire pixel segmentation using (1), (2), and (3)

Fig. 4. Fire pixel segmentation

positive classifications appeared (false alarms), which accounted for approximately 27%. After training the model, thirty other images with flames were randomly collected from the Internet and fed into the program for testing. All images were correctly classified.

$$accuracy = \frac{correct\ predictions}{\#\ of\ images} \times 100\% \quad (4)$$

The RGB color model is very popular for color cameras, color monitors, and color images. From the results it might be thought that this method would offer extremely accurate results. However, it was observed that false alarms occur in 27% for the cases of fire-like colors. It was difficult to distinguish between the fire pixels and the fire-like pixels in the RGB color model. One static characteristic that can assist in overcoming this problem is the luminance level of the pixel being considered. Unfortunately, the RGB color model represents both luminance and chrominance.

In order to obtain a higher accuracy, color and motion information can be combined. For instance, in order to distinguish between the fire pixels and fire-like pixels, the dynamic characteristics such as the motion, the changing area and other features of the flame region can be deployed to separate the foreground of the flame from the background.

This approach did not mention smoke detection. In many cases, fire in its early stages there may be no flames, but smoke is captured. Other criteria for smoke detection are needed due to the different color characteristics from those of the fire pixels.

The YCbCr Based Method

One of the primary color systems used to represent digital video component is the YCbCr color system. It represents color as the brightness and two-color difference signals, where Y is the luminance, Cb is blue minus luminance (B-Y) and Cr is red minus luminance (R-Y). Y is defined to have a nominal of 8-bit range of 16 to 235, but Cb and Cr have a nominal range of 16 to 240. An advantage of the YCbCr color system is separating the luminance from the chrominance more effectively than other color systems. For this reason, it is chosen to experiment its effectiveness on distinguishing fire pixels.

The performance of the proposed algorithm using the YCbCr color system to distinguish the fire pixels is tested on the same datasets using for verifying the RGB color system, two sets of images, one of which contains fire regions and the other containing different images with some of having fire-like regions.

The YCbCr Color Space Based Algorithm

In order to classify a pixel as a fire pixel utilizing the YCbCr color system, Figure 5 shows the flow chart of the proposed algorithm. It is based on the characteristics of the YCbCr color system. This YCbCr based approach has been followed due to its simplicity, effectiveness and wide range of use. In order to classify a pixel as a fire pixel, there are three rules that have to be satisfied. If a pixel satisfies these three rules, then it is considered to be a fire pixel.

Rule 1: YCbCr Intensity Values

After analyzing the color channels of many fire pixels, it has been noticed that fire color patterns have the Y values that are greater than the

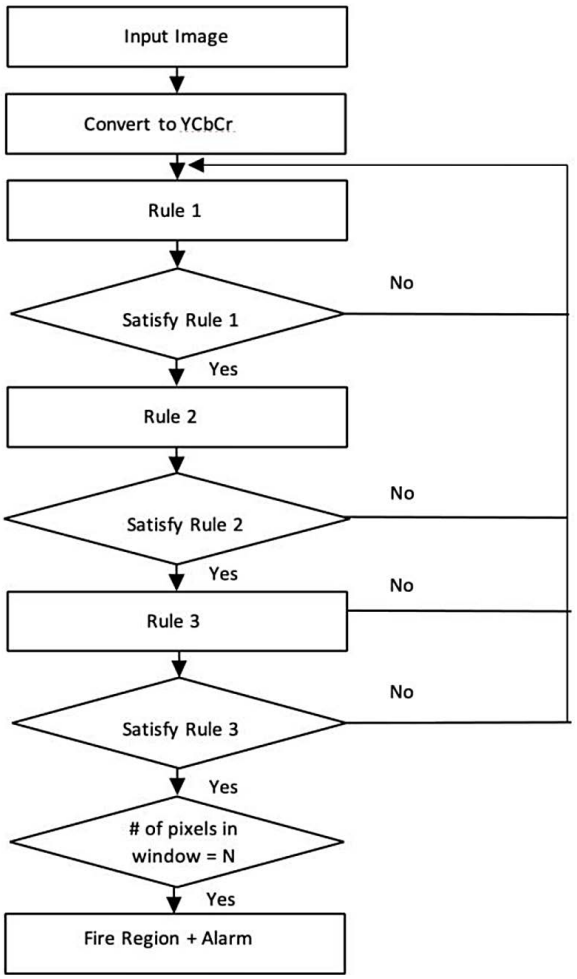

Fig. 5. Flowchart of the proposed method based on the YCbCr color model

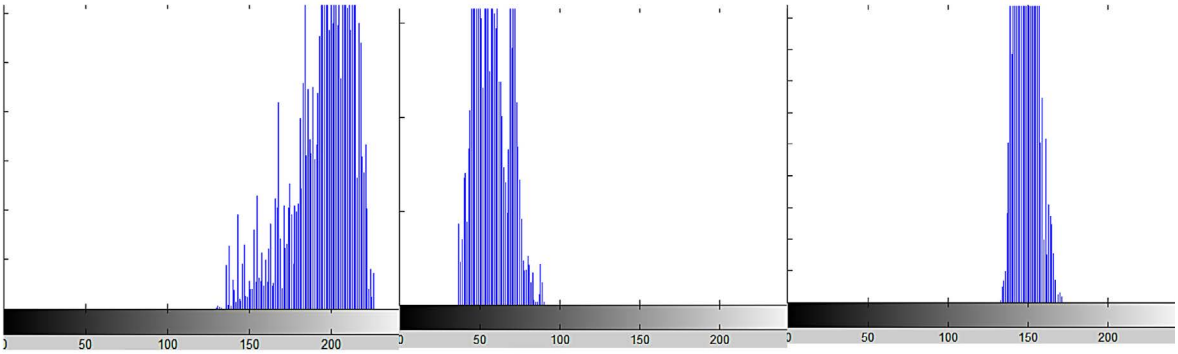

(a) Y channel (b) Cb channel (c) Cr channel

Fig. 6. Histogram of fire region

Cb, and Cr values that are greater than Cb. This can be observed from the histograms (Fig. 6) of Y, Cb and Cr of a fire region, respectively.

[11] observed this characteristic and mentioned that it was verified over countless experiments with images containing fire regions and formulated as the following rule:

$$F(x,y) = \begin{cases} 1, if\ Y(x,y) \geq Cb(x,y)\ and\ Cr(x,y)\ \geq\ Cb(x,y) \\ 0, otherwise \end{cases} \tag{5}$$

This can be considered as the first rule for detecting fire using the YCbCr color system. Fig. 7 shows the result of applying the first rule on some fire images from the considered dataset.

The first rule of detecting fire pixels operates efficiently when the background of the scene is dark; however, it misclassifies in the cases where the scene's background is bright.

Rule 2: Difference between the Cb and Cr Components of Fire Pixels

It can be noticed from Figure 8, that there is a significant difference between the Cb and Cr components of fire pixels. The Cb component is mainly "black" while the Cr component is mainly "white". This fact can be described as the following [7]:

$$F(x,y) = \begin{cases} 1, \text{if } |\text{Cb}(x,y) - Cr(x,y)| \geq \tau \\ 0, otherwise \end{cases} \tag{6}$$

Where the value of the threshold (τ) is observed from the established receiver operating characteristics (ROC) curve. It is obtained by experimenting different values of τ ranging from 1 to 100. The fire-pixel regions are manually segmented from each image. The true positive is

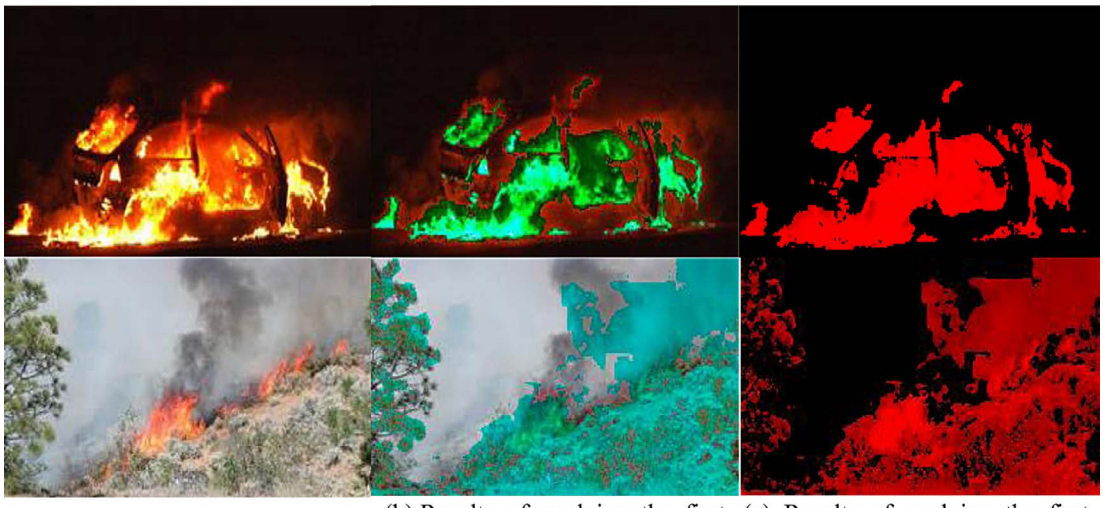

(a) Original fire images (b) Results of applying the first rule on (a) (c) Results of applying the first rule on (a)

Fig. 7. Results of applying the first rule

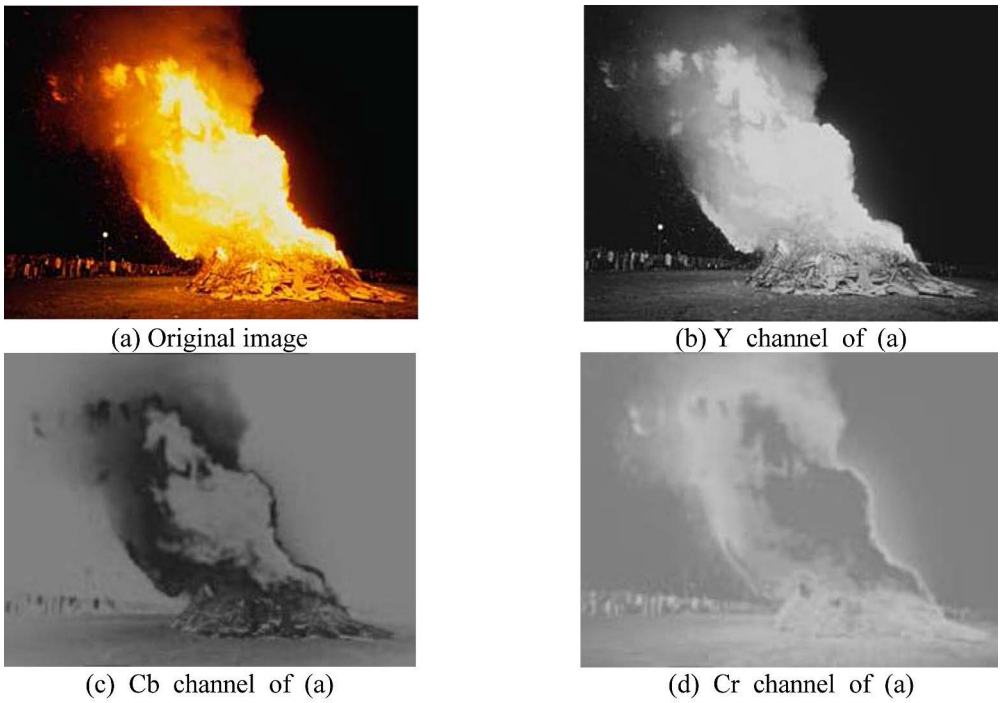

(a) Original image (b) Y channel of (a)

(c) Cb channel of (a) (d) Cr channel of (a)

Fig. 8. Y, Cb and Cr channels

defined as the decision when an image contains a fire, and false positive is defined as the decision when an image contains no fire but is classified as having fire. According to the research conducted by [7], the ROC curve consisted of 100 data points corresponding to different τ values, the corresponding correct-detection and false-alarm rates are computed and recorded. They determined the τ value to be 40 after carrying out the analysis on a set of 1000 images. [11] also applied the same method on 100 images and determined τ as being 70. In this work, different τ values ranging from 40 to 90 are tested on 50 images and it was observed that the best value for detecting the fire pixels was 70.

By applying the difference between the Cb and Cr components of the fire pixels (thresholding by $\tau = 70$) on some images from the dataset, the result of detecting the fire pixels is shown in [11].

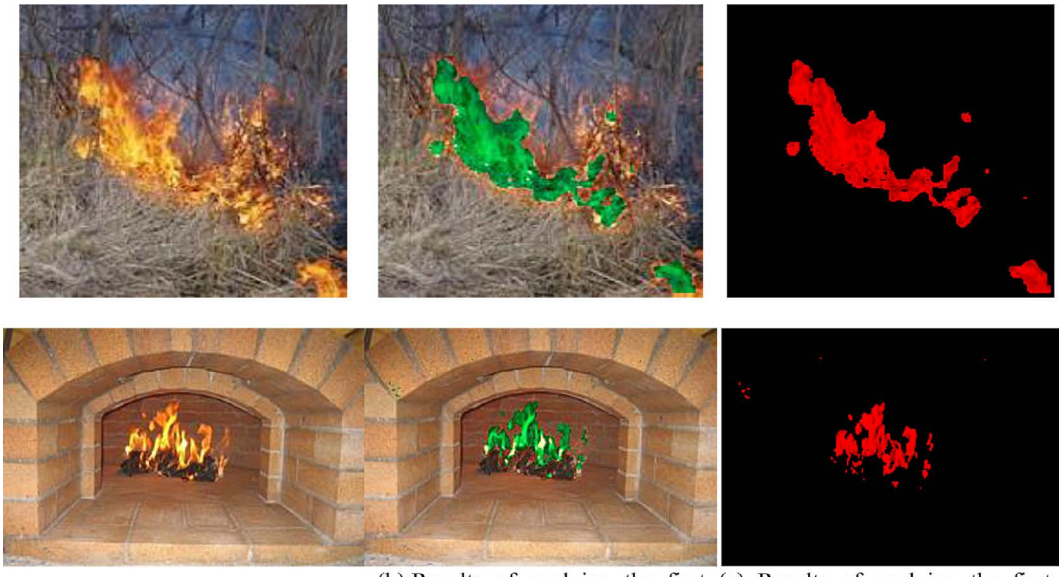

(a) Original fire images (b) Results of applying the first rule on (a) (c) Results of applying the first rule on (a)

Fig. 9. Results of applying the first rule

The thresholding rule is successful in detecting the fire pixels, but also misclassifies the fire-like pixels. That could result in increasing the false alarm rate in cases where no fire is present.

Rule 3: YCbCr Clusters

From the histogram analysis of fire regions, which are manually segmented, threshold values for the Y, Cb and Cr channels are defined. That has been accomplished by observing the histogram of thefire pixels for 50 images and recording the values of randomly selected fire pixels into a look-up table (Table 1). The look-up table was then converted into a graph and was divided into clusters (Fig. 10). After clustering, it can be observed that to consider a certain pixel as a fire pixel, it must have certain YCbCr value ranges for its pixels. The Y value was mostly less than 145 or greater than 170, the Cb was less than or equal to 120 and greater than or equal to 50, and the Cr channel had various values that were limited between 120 and 220. This condition is formulated by:

$$F(x,y) = \begin{cases} 1, \text{if } \mathrm{Y(x,y)} \geq 170 \mid \mathrm{Y(x,y)} < 145 \; and \; Cb(x,y) \leq 120 \\ Cb(x,y) \geq 50 \; and \; Cr(x,y) > 120 \\ Cr(x,y) < 220 \\ 0, otherwise \end{cases} \tag{7}$$

The result of applying that rule on some of the dataset images is shown in Figure 11. Although it detects the fire-like pixels, it is effective in detecting the fire regions and especially the flame edges of fire regions.

Results and Discussion of the YCbCr Algorithm

As it is unlikely to have a single pixel in an image to represent a fire region, for that a window of n-by-n pixels is used as a regulation to consider a certain region as a fire region. In

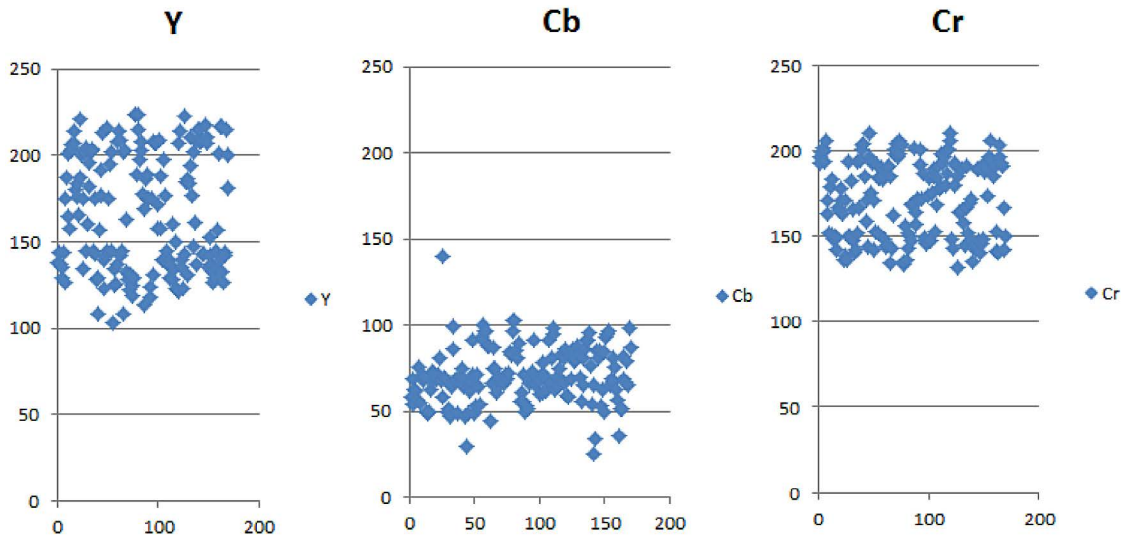

(a) Clusters of Y (b) Clusters of Cb (c) Clusters of Cr

Fig. 10. Clusters of Y, Cb and Cr

(a) Original fire image (b) Result of applying the third rule on (a) (c) Result of applying the third rule on (a)

Fig. 11. Result of applying the third rule

Table 1. Values of random Y, Cb and Cr pixels from 50 fire images

Y	Cb	Cr	Y	Cb	Cr	Y	Cb	Cr	Y	Cb	Cr
138	58	196	160	51	182	126	97	183	186	56	164
144	54	193	182	47	166	137	97	185	189	50	157
137	69	199	196	64	147	208	88	148	175	53	172
129	63	202	202	86	140	214	88	144	175	51	171
135	62	200	204	99	142	209	44	145	124	66	201
144	57	194	203	68	152	142	66	190	118	69	192
127	76	206	145	69	194	145	75	191	175	73	172
175	55	171	175	49	167	108	87	185	131	91	187
187	71	163	143	70	195	202	75	134	208	68	147
201	70	152	128	70	203	203	61	143	207	65	149
165	68	179	108	75	201	163	69	162	207	70	146
158	70	183	129	64	204	133	70	198	172	68	174
203	50	151	157	69	185	128	66	201	158	60	184
206	49	148	177	47	171	131	69	204	209	71	147
204	50	150	192	30	159	122	68	196	188	61	147
214	63	142	213	49	144	131	66	198	158	78	175
207	73	149	140	62	196	119	71	206	140	71	189
180	67	167	123	67	210	125	69	204	140	62	185
184	72	165	142	91	175	129	72	203	198	68	153
176	71	171	145	71	193	224	84	133	177	91	168
166	69	178	216	49	142	224	83	135	138	66	184
187	71	163	175	53	171	189	103	156	145	81	191
221	81	136	195	71	153	224	97	136	137	98	178
200	68	139	145	64	192	215	103	143	140	95	179
175	58	171	202	54	152	198	85	152	129	63	198
134	140	136	103	93	184	203	81	150	136	70	193
202	70	150	134	100	184	208	90	147	128	64	196
145	69	194	125	91	190	178	56	168	160	75	180
205	50	150	114	71	202	169	61	169	134	83	200
150	68	187	211	65	145	207	50	148	127	82	203
123	66	201	177	81	167	135	84	192	144	67	193
122	81	210	147	86	191	153	93	188	142	79	191
121	86	206	202	91	152	142	95	191	215	65	142
207	59	148	161	91	169	137	97	174	181	98	167
214	58	143	137	96	172	127	65	189	200	87	150
140	83	180	208	77	147	133	69	196	127	82	203
135	69	193	215	54	135	129	81	206	144	67	193
123	86	191	208	25	145	145	67	194	142	79	191
143	79	185	215	65	142	135	76	195	215	65	142
223	83	132	208	34	145	157	63	185	181	98	167
185	80	164	143	85	189	139	57	191	200	87	150
186	88	164	209	81	147	201	36	153	139	57	191
131	83	189	143	85	189	217	51	141	223	83	132
184	70	165	218	53	140	217	51	140	185	80	164
194	56	158	211	63	146	133	69	196	215	65	152

addition, by combining the three previously mentioned rules of detecting a fire pixel using YCbCr based system, Figure 12 and 13 illustrate the effect of each rule and the efficiency of all rules applied together on a certain image.

In order to evaluate the performance of the proposed algorithm, the dataset comprising 70 images which contain fire regions and 70 images containing the images with no fire regions and fire-like regions, was employed. Table 2 presents the confusion matrix for the predictions of the proposed algorithm.

$$accuracy = \frac{correct\ predictions}{\#\ of\ images} \times 100\% = \frac{120}{140} \times 100\% = 85.7\% \tag{8}$$

Table 2. Confusion matrix for the YCbCr proposed method

	Fire	No fire
Fire	70	0
No fire	20	50

The algorithm was able to detect 100% of the fire images in the provided dataset as containing fire, but for non-fire images its accuracy was 71.4%. The result gives a good impression on using the proposed YCbCr based algorithm on

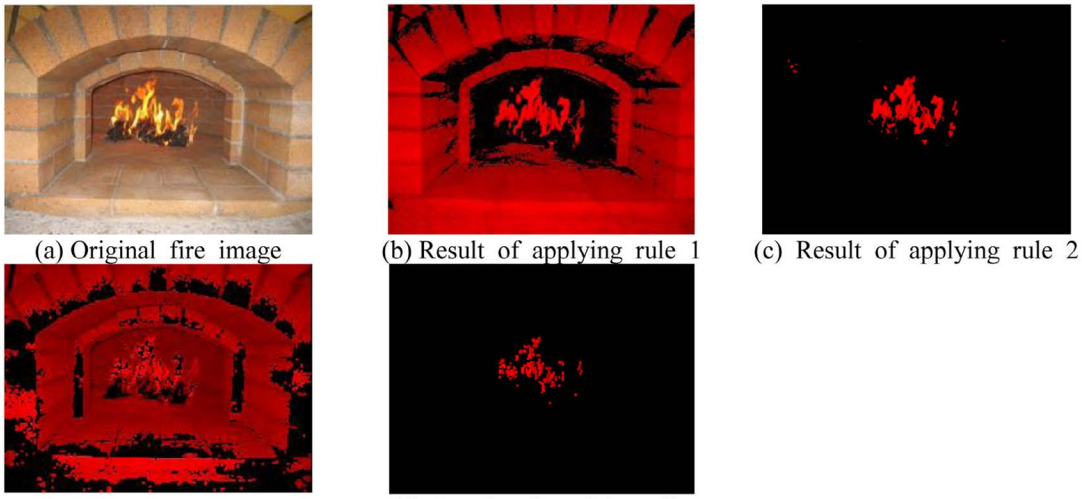

(a) Original fire image (b) Result of applying rule 1 (c) Result of applying rule 2

(d) Result of applying rule 3 (d) Result of applying all rules

Fig. 12. Result of applying the rules

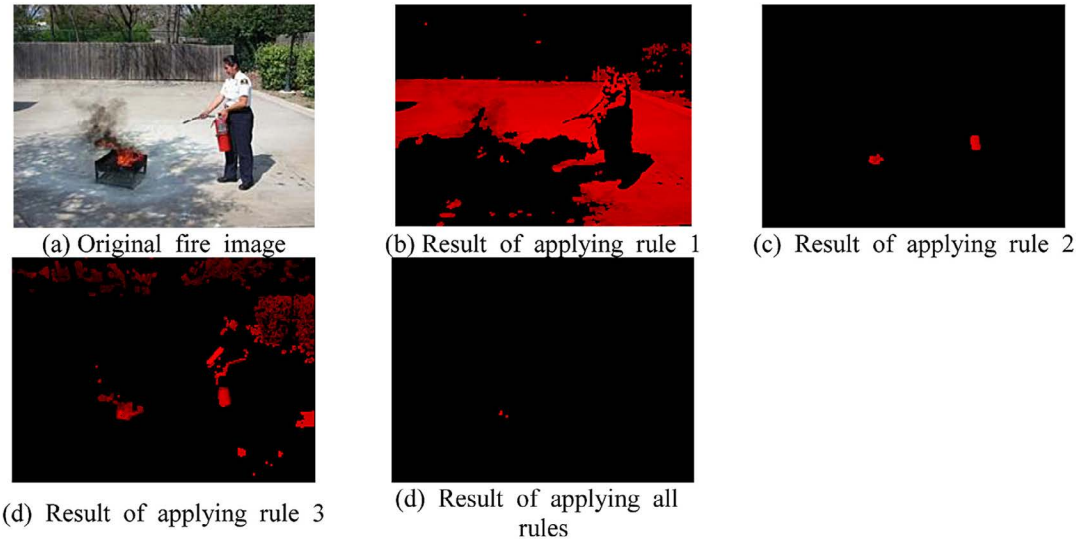

(a) Original fire image (b) Result of applying rule 1 (c) Result of applying rule 2

(d) Result of applying rule 3 (d) Result of applying all rules

Fig. 13. Result of applying the rules

promoting the safety issues. On the other hand, it gives false alarms in almost 28.6% with respect to the investigated dataset which will also have effects on other sides, as the expenses of evacuating. Moreover, it should be considered that the achieved accuracy included applying the algorithm on indoor and outdoor data set images with different environmental and weather conditions. In addition, the accuracy was achieved by only applying three simple and efficient rules. That requires less computation complexity which enables to use this algorithm in real-time fire detection.

The HSV Based Method

In this section, the details of detecting fire regions based on HSV color model are presented. Figure 14 indicates the flow chart of the approach in which the input RGB image is firstly converted to HSV color space. Next, the color values of each pixel are checked according to three HSV decision rules. The pixels satisfying the decision rules are further checked by Gaussian mixture model (GMM). Finally, some morphological postprocessing techniques are used on the detection result. The overall accuracy the dataset of the 140 images is 85.7%.

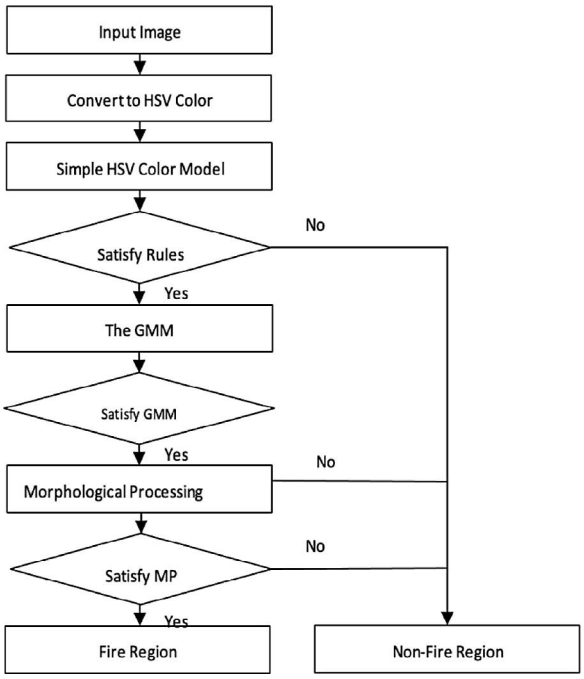

Fig. 14. Flowchart of the proposed method based on the HSV color model

The Three Decision Rules of the HSV Color Space Based Algorithm

Among various color systems, HSV (Hue, Saturation, Value) color model is very suitable for human interpretation, since hue, saturation and values components are intimately related to the way in which human beings perceive color. Empirically, the burning fire generally displays some obvious color features. For instance, the typical flame shows the white kernel, as well as red and yellow colors around the kernel.

On the basis of human interpretations of fire features, it is reasonable to assume that the flame color belongs to certain ranges of HSV components. In order to obtain the threshold values to separate flame color, the histograms shown in Fig. 15 were generated for fire pixels of HSV components. It can be concluded from these histograms that the fire pixels usually take much lower H values, but relatively higher S and V values. After a lot of experiments, the following decision rules to segment fire by HSV color space were defined:

$$\begin{aligned} &Rule\ 1\text{: } 0 \le H_{(x,y)} \le 0.35 \ \cup 3.0 \le H_{(x,y)} \le 3.14 \\ &Rule\ 2\text{: } 0.3 \le S_{(x,y)} \le 1.0 \\ &Rule\ 3\text{: } 0.8 \le V_{(x,y)} \le 1.0 \end{aligned} \tag{9}$$

As shown in Figure 16, the above inequalities are applied to generate some binary maps which indicate whether the pixel located at

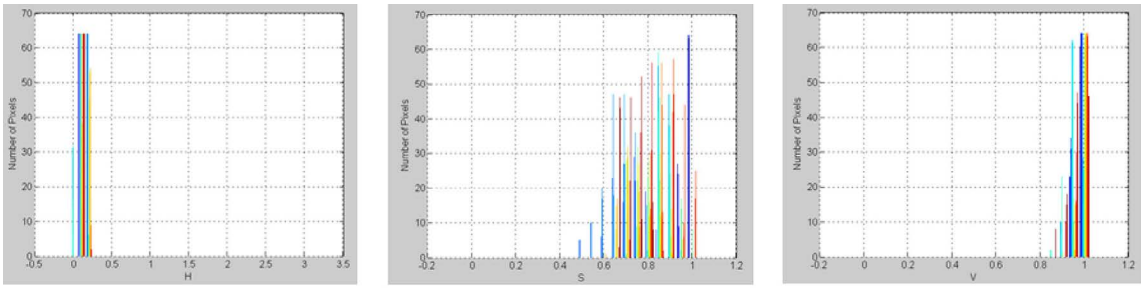

(a) H component histogram (b) S component histogram (c) V component histogram

Fig. 15. The fire pixels histograms

spatial location (x, y) is classified as fire (binary value of 1) or non-fire (binary value of 0) pixel. Specially, Figure 16(a) is the input image of hay fire; Figure 16(b) shows the fire detection result after using Rule 1, which not only segments the fire region but also incorrectly takes the color of hay as the fire pixels. After combining Rule 1 and Rule 2, the fire detection result provided in Figure 16(c) has been improved to some extent, although the result is still not satisfactory. When combining three decision rules together, a good visual result is obtained in Figure 16(d) in which almost all the fire regions in Figure 16(a) have been segmented correctly.

Although the above three decision rules show effectiveness in separating fire regions in some images, just using those simple inequalities tend to fail distinguish fire and objects with fire-like colors. This is because those three decision rules only define rough color ranges for flame, and some other fire-like colors are included in those ranges as well. Figure 17(a) shows an image with reddish color, while Figure 17(b) is the segmentation result using above three rules. Apparently, all the fire-like colors in Figure (a) are mistakenly taken as fire regions.

Gaussian Mixture Model Based Fire Detection

Since using only simple mathematical formulations in HSV color space to differentiate between the fire and fire-like colors is impossible, it is necessary to explore more accurate fire color models to represent the fire pixels distribution. As shown in Figure 18, 1024 fire pixels segmented manually from fire images are plotted in 3D space. In order to more precisely represent the 3D shape of the point cloud in Figure 18, Gaussian mixture model (GMM) is applied in this work, thus the pixel the color of which is within the range of GMM distribution model can be regarded as a candidate flame pixel.

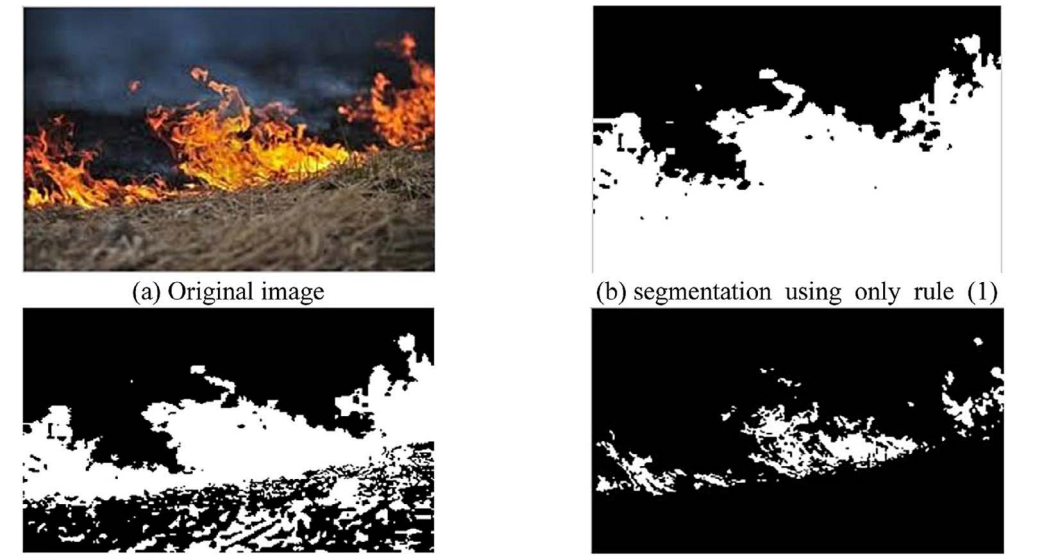

(a) Original image (b) segmentation using only rule (1)

(c) segmentation using rules (1) and (2) (d) segmentation using rules (1), (2) and (3)

Fig. 16. Fire pixels segmentation

(a) Original image (b) The detection result

Fig. 17. Fire-like color detection using decision rules

Gaussian Mixture Model

Assume there are M single Gaussian models that describe sampled fire pixels, and each single Gaussian model takes the proportion as $a_j (1 \leq j \leq M)$, the probability density function (p.d.f) of an observation x_i belonging to the defined GMM can be represented by the following equation:

$$p(x_i) = \sum_{j=1}^{M} a_j N_j(x_i;\ \mu_j, \Sigma_j) \tag{10}$$

where: $a_j (1 \leq j \leq M)$ is the mixing parameter, $N_j(x_i; \mu_j, \Sigma_j)$ is the j_{th} single Gaussian model.

They are expressed as:

$$\sum_{j=1}^{M} a_j = 1 \tag{11}$$

$$N_j(x_i; \mu_j, \Sigma_j) = \frac{1}{\sqrt{(2\pi)^m |\Sigma_j|}} exp\left[-\frac{1}{2}(x_i - \mu_j)^T \Sigma_j^{-1}(x - \mu_j)\right] \tag{12}$$

where: μ_j is the mathematical expectation of the j_{th} model, Σ_j is the covariance of the j_{th} model. In order to describe fire pixels distribution in 3D space by the GMM, the main premise is to ascertain the unknown parameters M, a_j, μ_j, and Σ_j. The number (M) of single Gaussian models can be manually assigned or obtained by the trial-and-error method. In this work, eight single Gaussian models were chosen after multiple experiments. For the other three unknown parameters, they can be estimated by the expectation maximization (EM) algorithm discussed in the following section.

Estimating Parameters Using EM Algorithm

There are various approaches that can be used for determining the parameters of the GMM from a set of initial data Hirsch (2004). In this work, the expectation maximization (EM) algorithm is deployed for the GMM parameters estimation.

Regarding to the GMM in equation (10), assume that $\theta_j = (a_j, \mu_j, \Sigma_j)$ and $\Phi = (\theta_1, \ldots \theta_M)^T$, the log-likelihood for the data set $X = \{x_i | 1 \leq i \leq N\}$ is given by:

$$l((X|\Phi)) = log \prod_{i=1}^{N} \sum_{j=1}^{M} a_j N_j(X; \mu_j, \Sigma_j) = \sum_{i=1}^{N} log \sum_{j=1}^{M} a_j N_j\,(x_i; \mu_j, \Sigma_j) \tag{13}$$

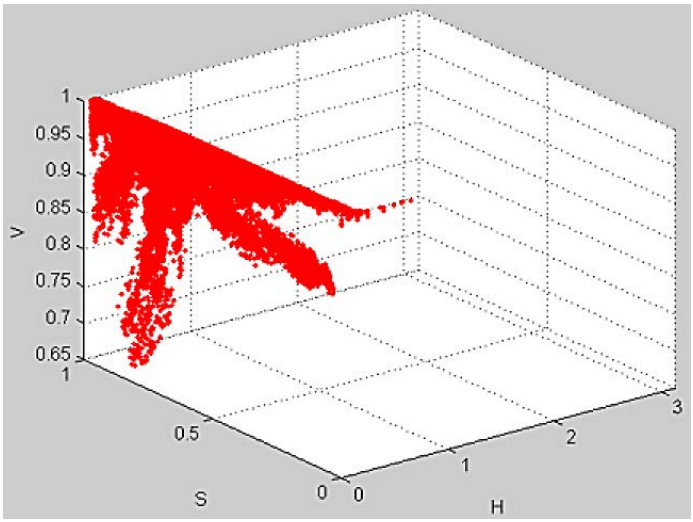

Fig. 18. 3D point cloud of sampled fire pixels

When the value of $|l(X|\Phi) - l(x|\Phi)'|$ is continually minimized, such that it is less than a threshold value ε, for example 10^{-5} the GMM is converged. However, the EM algorithm should start with some initial guess for the parameters of the GMM. In this work, initialization of the mathematical expectation μ_{j_0} and the covariance Σ_{j_0} of the model through K-means clustering method, and the mixing parameter a_{j_0} was computed based on the clustering result. According to the initial guess for the GMM unknown parameters, the posterior probability for $a_j (1 \le j \le M)$ is computed as:

$$\beta_j = E\left(\left(a_j \middle| x_i; \Phi\right)\right) = \frac{a_j N_j(x_i; \Phi)}{\sum_j^M a_j N_j(x_i; \Phi)}, 1 \le i \le N, 1 \le j \le M \tag{14}$$

After computing the posterior probability β_j, the values of parameters a_j, μ_j, Σ_j are be updated by:

$$a_j' = \frac{\sum_i^N \beta_{ij}}{N} \tag{15}$$

$$\mu_j' = \frac{\sum_{i=1}^N \beta_{ij} x_i}{\sum_{i=1}^N \beta_{ij}} \tag{16}$$

$$\Sigma_j' = \frac{\sum_{i=1}^N \beta_{ij}\left(x_i - \mu_j'\right)\left(x_i - \mu_j'\right)^T}{\sum_{i=1}^N \beta_{ij}} \tag{17}$$

Using the updated parameters , the value of could be computed iteratively until the GMM is converged. Then, whether one pixel belongs to fire region of the image being processed can be determined by computation of its probability with (10).

Morphological Post-Processing

The approach of combining the HSV decision rules and the GMM works relatively well in distinguishing the fire and fire-like colors, but some issues still exist. For example, some isolated fire-like pixels may be still incorrectly taken as the fire pixels (Figure 21(c)), and not all fire pixels are segmented from the image (Figure 20(c)). In order to further enhance the algorithm, morphological processing techniques are adopted to improve the fire detection results. Firstly, the number of the fire pixels in each connected component is calculated. Only when the number of pixels is greater than the predefined threshold like 20, can the component be regarded as the fire region. In addition, morphological opening and closing operations can be utilized to fill some possibly existing holes in the detected fire regions.

HSV model Experimental Results

The HSV color space based fire detection mainly involves three parts: simple HSV color decision rules, GMM and morphological post-processing. Before using GMM, manual segmentation of fire samples and considering them as training data. As shown in Figure 20, 1024 fire pixels are applied to estimate the unknown parameters of the GMM by the EM algorithm.

Figure 20 shows an example of fire detection using the proposed algorithm, in which Figure 20(a) is the input fire image, Figure 20(b) is the detection result under three decision rules of HSV color model. Clearly, the detection result by the simple HSV color model is not satisfied, since a lot of fire-like pixels such as the color of smoke and red house are incorrectly taken as flames. Figure 20(c) indicates the fire regions detected by the HSV color model and GMM, while Figure 20(d) is the final result after the morphological post-processing. It can be seen that GMM is more robust in distinguishing fire and fire-like colors than the decision rules of the HSV color model. Especially, the relatively good result was obtained after filling holes in the fire regions.

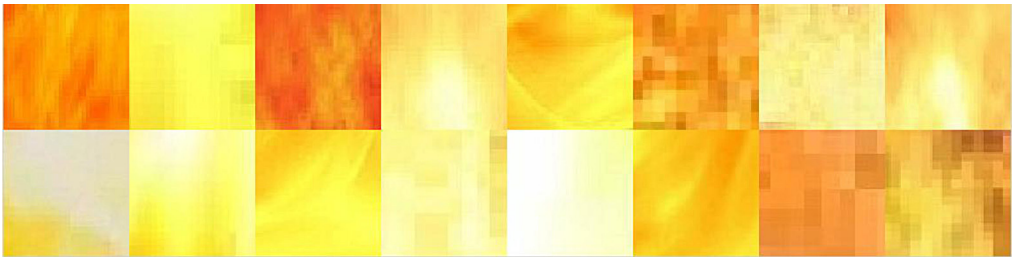

Fig. 19. Training samples segmented from real fire images

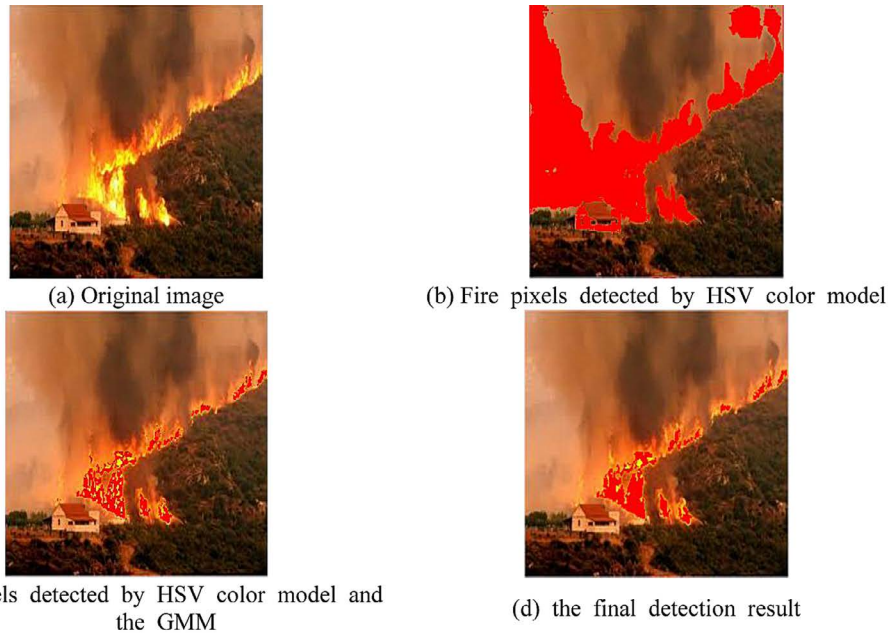

(a) Original image (b) Fire pixels detected by HSV color model

(c) fire pixels detected by HSV color model and the GMM (d) the final detection result

Fig. 20. Fire regions segmentation

Further examples of successful detecting non-fire colors are shown in Figure 21, the original input image of Figure 21(a) contains the red and yellow color with high illumination, which has the high similarity with the fire color. Without doubt, the decision rules based on a simple HSV color model misclassifies many regions as the fire pixels which are shown as binary "1" in Figure 21(b). Even worse, there are still some isolated pixels that are detected as the fire pixels by the trained GMM (Fig. 21(c)). After adding another constraint that the number of pixels in the fire regions should be greater than the predefined threshold, the correct classification result is successfully gained, which is shown in Figure 21(d).

During the simulations, the algorithm was tested on real-world images that are taken from a random selection on Internet. As previously mentioned for the RGB and YCbCr color models, the collected images were divided into two groups, namely the fire and non-fire group, and each group had 70 images. In the fire group, it consisted of different types of

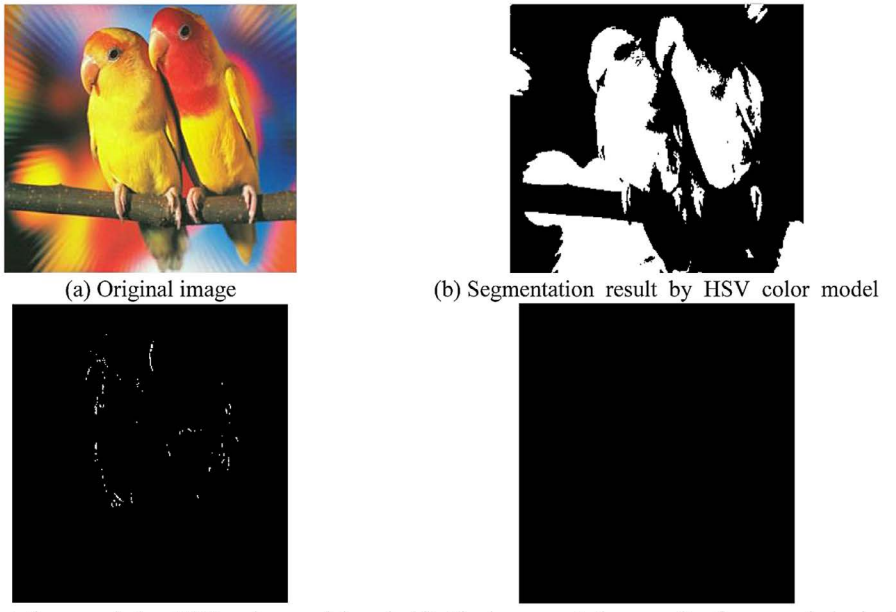

(a) Original image (b) Segmentation result by HSV color model

(c) Segmentation result by HSV color model and the GMM (d) Final segmentation result after morphological post-processing

Fig. 21. Fire-like colors segmentation

fires such as forest fire and residential fire. Besides, the images were captured at day time or night time to evaluate the algorithm performance under different lighting conditions. In the non-fire group, it consisted of the objects with fire-like colors such as red trunk and sun. (Table 3) shows the detection results of our algorithm on the fire and non-fire images, in which the first column is the sequence numbers of images in each group, and the "1" in the other two columns means fire alarming, but "0" represents no fire in the detected image.

As indicated by Table 3, the accuracies of the algorithm shown in (Table 4), in which the accuracy for fire group is much higher, 91.4%, and the accuracy for the non-fire group is relatively lower, 80.0%. The overall accuracy for both groups is 85.7%. The relatively lower accuracy on non-fire images is mainly due to too many images in the non-fire group having fire-like colors.

CONCLUSIONS

This work presented three intelligent approaches to detect fires based on three different color models: RGB, YCbCr and HSV. The accuracy of approximately 86% was achieved by applying the three approaches to the data set consisting of 140 images, which had been captured indoor and outdoor under different environmental and weather conditions. In addition, each technique deployed three simple but efficient rules, which requires less computation complexity. These two advantages enable the algorithms to be used in real-time fire detection. The RGB and YCbCr methods were able to detect 100% of the cases on the fire image set. The HSV adopted the Gaussian mixture model (GMM). In turn, the expectation maximization (EM) algorithm presented the best results on the fire-free images by predicting 80%

Table 3. The detection results on fire and non-fire images

Number	Fire	Non-Fire	Number	Fire	Non-Fire	Number	Fire	Non-Fire
1	1	0	25	1	0	49	1	1
2	1	1	26	1	0	50	1	0
3	1	0	27	1	0	51	1	1
4	1	1	28	1	1	52	1	0
5	1	0	29	1	0	53	1	0
6	1	0	30	1	0	54	1	0
7	1	0	31	1	0	55	1	0
8	1	1	32	1	0	56	1	0
9	1	1	33	1	0	57	1	0
10	1	0	34	1	1	58	1	0
11	0	0	35	1	0	59	1	0
12	1	0	36	1	0	60	1	0
13	0	0	37	1	0	61	1	0
14	1	1	38	1	0	62	1	0
15	1	0	39	1	0	63	1	0
16	1	0	40	1	0	64	1	0
17	1	0	41	1	0	65	1	0
18	1	1	42	1	0	66	1	0
19	1	0	43	0	0	67	0	0
20	1	1	44	1	0	68	1	0
21	1	1	45	1	0	69	1	0
22	1	1	46	1	0	70	1	0
23	1	1	47	1	0			
24	0	0	48	0	0			

Table 4. The accuracies of utilizing the HSV color model

Test data	Correct detection	Total number	Accuracies
Fire group	64	70	91.4%
Non-Fire group	56	70	80.0%

of the images without fire. There was a trade-off between the accuracy of detecting the fire regions precisely and the probability of detecting the fire-like regions. In order to improve the reliability of the presented techniques, dynamic characteristics of flame such as flame motion and geometry are to be integrated in the future.

REFERENCES

1. Yu C. Mei Z. Zhang X. A Real-Time Video Fire Flame and Smoke Detection Algorithm. Procedia Engineering. 2013;62:891–898. DOI: 10.1016/j.proeng.2013.08.140
2. Gong F., Li C., Gong W., Li X., Yuan X., Ma Y., Song T. A Real-Time Fire Detection Method from Video with Multifeature Fusion. Computational Intelligence and Neuroscience. 2019;1687-5265. DOI: 10.1155/2019/1939171
3. Töreyin B., Dedeoglu,Y., Gudukbay U., Cetin A. Computer Vision Based Method for Real-Time Fire and Flame Detection. Pattern Recognition Letters. 2005;27:49–58. DOI: 10.1016/j.patrec.2005.06.015
4. Appana D., Islam R., Khan S., Kim J. A Video-Based Smoke Detection Using Smoke Flow Pattern and Spatial-Temporal Energy Analyses for Alarm Systems. Information Sciences. 2017;418-419:91-101, DOI:10.1016/j.ins.2017.08.001
5. Celik T. Fast And Efficient Method for Fire Detection Using Image Processing. ETRI Journal. 2010;6:881–890. DOI:10.4218/etrij.10.0109.0695
6. Hsu T., Pare S., Meena S., Jain D., Li D., Saxena A., Prasad M., Lin C. An Early Flame Detection System Based on Image Block Threshold Selection Using Knowledge of Local and Global Feature Analysis. Sustainability. 2020;12(21):1-22. DOI:10.3390/su12218899
7. Celik T., Demirel H., Ozkaramanli H., Uyguroglu M. Fire Detection Using Statistical Color Model in Video Sequences. Journal of Visual Communication and Image Representation. 2007;18:176–158. DOI:10.1016/j.jvcir.2006.12.003
8. Yu Z., Xu Y., Yang X. Advances in multimedia modeling, Springer, Berlin Heidelberg. 2010;477–488.
9. Tong X., Li R., Ge L., Zhao L., Wang K. A New Edge Patch with Rotation Invariance for Object Detection and Pose Estimation, Sensors. 2020;20(3):887. DOI:10.3390/s20030887
10. Li Y., Wu W. Sequential Pattern Technology for Visual Fire Detection. Journal of Electronic Science and Technology. 2012;1:276–280. DOI:10.3969/j.issn.1674-862X.2012.03.014
11. Vipin V. Image Processing Based Forest Fire Detection. International Journal of Emerging Technology and Advanced Engineering. 2012;2:87–95. DOI:10.1155/2018/7612487
12. Valikhujaev Y., Abdusalomov A., Cho Y.I. Automatic Fire And Smoke Detection Method for Surveillance Systems Based on Dilated CNNs. Atmosphere. 2020;11(11):1241. DOI: 10.3390/atmos11111241
13. Hirsch R. Exploring colour photography: A complete guide. Laurence King, London, UK. 2004.
14. Yang M.H., Ahuja A. Gaussian mixture model for human skin color and its applications in image and video databases. Proceedings of Storage and Retrieval for Image and Video Databases Engineering (SPIE 99). 1999;3656:458–466.
15. Varma S., Behera V. Human Skin Detection Using Histogram Processing and Gaussian Mixture Model Based on Color Spaces. ICISS. 2017;116-120.